Cloud Layer Thicknesses from a Combination of Surface and Upper-Air Observations

KIRK D. POORE*

AVION, Incorporated, Bridgeton, Missouri

JUNHONG WANG

Department of Geological Sciences, Columbia University, New York, New York

WILLIAM B. ROSSOW

NASA Goddard Institute for Space Studies, New York, New York

(Manuscript received 10 November 1993, in final form 11 July 1994)

ABSTRACT

Cloud layer thicknesses are derived from base and top altitudes by combining 14 years (1975–1988) of surface and upper-air observations at 63 sites in the Northern Hemisphere. Rawinsonde observations are employed to determine the locations of cloud-layer top and base by testing for dewpoint temperature depressions below some threshold value. Surface observations serve as quality checks on the rawinsonde-determined cloud properties and provide cloud amount and cloud-type information. The dataset provides layer-cloud amount, cloud type, high, middle, or low height classes, cloud-top heights, base heights and layer thicknesses, covering a range of latitudes from 0° to 80°N. All data comes from land sites: 34 are located in continental interiors, 14 are near coasts, and 15 are on islands. The uncertainties in the derived cloud properties are discussed. For clouds classified by low-, mid-, and high-top altitudes, there are strong latitudinal and seasonal variations in the layer thickness only for high clouds. High-cloud layer thickness increases with latitude and exhibits different seasonal variations in different latitude zones: in summer, high-cloud layer thickness is a maximum in the Tropics but a minimum at high latitudes. For clouds classified into three types by base altitude or into six standard morphological types, latitudinal and seasonal variations in layer thickness are very small. The thickness of the clear surface layer decreases with latitude and reaches a summer minimum in the Tropics and summer maximum at higher latitudes over land, but does not vary much over the ocean. Tropical clouds occur in three base-altitude groups and the layer thickness of each group increases linearly with top altitude. Extratropical clouds exhibit two groups, one with layer thickness proportional to their cloud-top altitude and one with small ($\leq$1000 m) layer thickness independent of cloud-top altitude.

1. Introduction

Cloud variations affect earth's climate by modulating the radiation field (e.g., Stephens and Webster 1984). Earth and surface radiation budgets (ERB and SRB) strongly depend on cloud optical properties, their horizontal distribution (cloud cover), and their vertical distribution (cloud-top and/or cloud-base temperature or height). Cloud-base temperature is an important determinant of the surface net longwave flux (Fung et al. 1984; Stephens and Webster 1984; Rossow and Lacis 1990); an uncertainty of 100 mbar in the base pressure of midlevel clouds translates into an uncertainty in surface net longwave radiation of at least 10 Wm^{-2} (Fung et al. 1984); larger uncertainties occur for smaller changes in lower-level cloud-base heights. Variation of net longwave flux at the top of the atmosphere is a stronger function of the cloud-top temperature (or height) (Stephens and Webster 1979; Arking 1991). Both ERB and SRB also depend on cloud optical thickness, which is affected by cloud physical thickness (Stephens and Webster 1984; Curry et al. 1990; Tselioudis et al. 1992).

The horizontal and vertical distributions of clouds directly force atmospheric motions by altering gradients of the total diabatic heating/cooling composed of radiative heating/cooling and latent heat release (Webster and Stephens 1984). Stephens and Webster (1981) show that low-level clouds radiatively cool the local atmosphere, but that this cooling decreases or even changes to heating as cloud-base rises. Houze (1982) has suggested that the total disturbance scale and vertical distribution of diabatic heating in convective systems are substantially altered by the cloud-modified

* Formerly USAF Environmental Technical Application Center, Scott AFB, Illinois.

Corresponding author address: Ms. Junhong Wang, Atmospheric and Planetary Science Program, Columbia University, NASA/GISS, 2880 Broadway, New York, NY 10025.

radiative heating and the resultant upper-level release of latent heat (cf. Machado and Rossow 1993). However, clouds are also a consequence of atmospheric motions, so that their vertical structure is also diagnostic of cloud formation processes and the atmospheric circulation. Betts (1989), for example, suggested that, since boundary layer dynamics determines cloud thickness, observations of cloud properties can be used to estimate the dynamical processes in clouds, such as the mean divergence, entrainment rate, and radiative cooling.

Climate and weather GCM calculations need to link the ERB and SRB in cloudy conditions to atmospheric motions and then to cloud properties, but this requires specification of more than the vertically averaged cloud properties. The GCMs must also account for the vertical structure and distribution of cloud layers and cloud-layer overlap (e.g., Morcrette and Fouquart 1986).

Considerable efforts have been devoted to establishing global cloud climatologies [see Hughes (1984) for a review of older climatologies]. Surface weather observations provide total cloud cover, cloud amount by morphological type, estimated base height of the lowest clouds, and frequency distributions of occurrence and co-occurrence of different morphological cloud types (Hahn et al. 1982, 1984; Warren et al. 1985, 1986; Warren et al. 1988). However, surface observers have more difficulties identifying altostratus/altocumulus and cirrus clouds reliably, particularly at night or when lower clouds are present. Surface observations also do not provide any information on cloud-top height or optical thickness. The International Satellite Cloud Climatology Project (ISCCP) reports global distributions of cloud amount, cloud-top temperature/pressure, and optical thickness (Rossow and Schiffer 1991). The *Nimbus-7* cloud climatology provides information on cloud altitude distributions and cloud amount (Stowe et al. 1989). Both of these satellite datasets have a partially obscured view of low-level clouds and larger uncertainties in determining the heights of thinner cirrus because it is common for two or more clouds to occur simultaneously over the same location but at different altitudes (Warren et al. 1985; Tian and Curry 1989). The Stratospheric Aerosol and Gas Experiment, observing solar occultations, scans downward through the atmosphere with much higher sensitivity and determines the vertical extent and frequency of occurrence of the highest cloud-tops, including the thinner cirrus clouds near the tropopause (Woodbury and McCormick 1986; Liao et al. 1995a, 1995b). Satellites, however, have difficulties reliably detecting boundary layer cloudiness because of obscuration by upper-level clouds and cannot determine cloud-base locations or vertical layer distributions.

Thus, although the distribution of cloud-top altitudes and low cloud-base heights are well but separately observed, there are very few studies that correlate cloud-top and base locations to determine cloud layer thicknesses and describe cloud-layer overlaps or the vertical distribution of cloud water and ice. One study is that of Bary and Möller (1963), which only extends up to a 5-km altitude. The United States Air Force 3D Nephanalysis combines satellite and surface observations to determine cloud occurrence in three layers (high, middle, low), which provides some information on multiple layers [see January and July 1979 results in Henderson-Sellers (1986)]. Cloud overlap statistics were analyzed for January 1979 over the North Atlantic Ocean (Tian and Curry 1989). The only study of cloud-layer thickness is of cirrus clouds at 11 weather stations in the former USSR (Izumi 1982). A large number of cloud field experiments have been conducted over the past several decades and the collection of the results of these case studies do provide some indication of cloud vertical structures (cf. Cotton and Anthes 1989). However, statistically complete information about cloud-base heights of middle and high clouds, cloud-layer thicknesses at all levels, and the structures of multilayer clouds remains a significant gap in current cloud climatologies.

Surface lidars (Sassen 1991) and millimeter wavelength radars (Kropfli et al. 1995) are valuable for profiling clouds, particularly when used together; however, they can only be operated at a few sites and cannot provide global coverage. In the near future, there are no plans to fly an instrument on a satellite that can provide information on cloud vertical structure, though a profiling radar has been proposed (WCRP-84 1994). A merged analysis of High-Resolution Infrared Radiation Sounder and Advanced Very High Resolution Radiometer data may provide some indications of the presence of two layers (Baum et al. 1994); even more information could be obtained from an infrared spectrometer (e.g., Carlson et al. 1993). Estimates of cloud physical thickness have also been estimated from satellite-measured optical thicknesses for certain cloud types in field experiments (Minnis et al. 1992).

The vertical profiles of temperature and humidity measured by rawinsondes as they penetrate cloud layers also reflect some aspects of the vertical distribution of clouds. Poore (1991) had already combined rawinsonde and surface observations to determine cloud-layer thicknesses. Since this source of information about cloud vertical distributions is unexploited, we examine these first results to determine whether an analysis of the whole rawinsonde archives is warranted as the first step in assembling a climatology of cloud-layer information. The dataset, analysis method, error sources, and possible analysis improvements are discussed in section 2. These first results provide a first approximation to a climatology of cloud layer thicknesses, base heights, and top heights; however, there are some significant limitations that are discussed in section 3. We also discuss comparisons of cloud-base heights with surface estimates and cloud-top heights

with satellite measurements. The derived latitudinal and seasonal variations of cloud- (and clear) layer thicknesses, as well as relations among top height, base height, and layer thickness, are presented in section 4 and discussed in section 5.

2. Data and analysis method

a. Data description

The locations of moist (presumably cloudy) layer base and top are determined from rawinsonde observations (RAOBS) of temperature and humidity (expressed as dewpoint temperature) from the surface to 35 000 ft (10 668 m) or the height at which the temperature falls below −40°C, whichever is lower. The original RAOBS are linearly interpolated to 250 ft (76 m) intervals because many do not report all significant levels. When too few significant levels are reported, too many moist layers start or end at the mandatory levels, which produces spuriously high frequency peaks or "spikes" in the vertical distributions of cloud-base and top. Interpolation smoothes out these spikes. Since RAOBS dewpoint temperature determinations are usually unreliable at temperatures below −40°C, the RAOBS profiles are cut off at the last nonmissing values when a temperature of −40°C is reached below a height of 35 000 ft above ground level (AGL).

Surface weather observations (SWOBS) at the same site provide information on clouds, consisting of total cloud-cover fraction, fractions of the standard morphological cloud types, including high, middle, and low height classes, estimates of the base height AGL of each cloud height class, and a present weather code. SWOBS are used to verify the RAOBS-determined moist-layer properties. The standard cloud types are converted to the same simpler cloud-type codes used by the Real Time Nephanalysis model, in which clouds are grouped into 10 types (Table 1).

RAOBS and SWOBS from 63 sites in the Northern Hemisphere were processed to obtain the cloud-layer thickness climatology. Only 0000 and 1200 UTC observations were used. Thirty-four sites located well inland are used to produce a continental climatology; 15 sites on islands and 14 at the coast are used to produce an oceanic climatology. Most sites have records 14 years long (1975–1988), but a few have shorter records.

b. Analysis method

Cloud-base and cloud-top heights AGL are determined by combining RAOBS and SWOBS. The RAOBS vertical profile of dewpoint depression (ΔT_d)[1] the difference between temperature and dewpoint temperature) indicates possible moist layers by values below some threshold. The locations at which ΔT_d crosses the threshold value indicate the layer base and top. The presence of a cloud in the moist layer, as well as its approximate height, is verified by comparison to the SWOBS cloud-layer report.

TABLE 1. Cloud-type codes reported and six classifications used.

Code	Cloud Type	Simple Classification
1	Cb Cumulonimbus	Cb
2	St Stratus	St
3	Sc Stratocumulus	St
4	Cu Cumulus	Cu
5	As Altostratus	As
6	Ns Nimbostratus	Ns
7	Ac Altocumulus	As
8	Cs Cirrostratus	Ci
9	Cc Cirrocumulus	Ci
10	Ci Cirrus	Ci

The ΔT_d thresholds used are a modification of those recommended by AWS (1979): 2°C at temperatures above 0°C, 4°C at temperatures between 0 and −20°C, and 6°C at temperatures below −20°C. These values are consistent with an extensive analysis of one year of RAOBS data from Oklahoma City; Andersen Air Force Base (AFB), Guam; and Osan AFB, Korea, which shows that slightly reduced thresholds of 1.7°, 3.4°, and 5.2°C for the same temperature ranges produce the largest frequency of matches with surface observations. Cloud-base, cloud-top, and cloud-layer thickness are determined for each moist layer in the RAOBS profile, and a height class is assigned according to the layer base height AGL: bases at or below 6500 ft (1981 m) are called low clouds, between 6500 ft and 16 500 ft (5029 m), middle clouds, and above 16 500 ft, high clouds.

The RAOBS moist layers are compared with the SWOBS cloud layers at the same site, date, and time and in the same height class, and then final RAOBS/SWOBS cloud layers are reported. Sometimes there is no match, for example, when a midlevel RAOBS moist layer does not have a corresponding SWOBS midlevel cloud layer. Unmatched cloud layers are discarded. There are also some mismatches, for example, when the surface observer reports low cloud while the RAOBS reports middle cloud. Mismatched cloud layers are also removed. The percentage of unmatched and mismatched cases and reasons for them are discussed in the next section. Matched cloud layers are checked further and some corrections made: 1) low cloud-layer thicknesses are required to be >100 ft (30 m) and middle and high cloud layer thicknesses >200 ft (61 m); 2) if two moist layers are found, where only one cloud layer is observed from the surface, the RAOBS layer closer to the SWOBS cloud height is kept and the other discarded; 3) moist layers that extend to the top of the

[1] Dewpoint depression is the difference between temperature and dewpoint temperature and is an alternative way to represent relative humidity (ΔT_d = 0 at 100% relative humidity). We use this form because most RAOBS humidity data are reported as dewpoint temperatures.

RAOBS profile are discarded because they have indeterminate top heights AGL; and 4) if the RAOBS moist layer starts at or near the surface, because of rain or fog, then the base height AGL is taken from SWOBS because cloud-bases below 3000 ft AGL (914 m) are usually reliably measured.

c. Error assessment

Theoretically, the dewpoint temperature (T_d) equals the air temperature (T) in a cloud. Finite positive ΔT_d thresholds must be chosen to indicate cloud layers because of 1) the existence of real but small differences between T and T_d when the cloud is not in equilibrium, as may occur in strong updrafts, 2) the increasing difference between frost point and dewpoint as temperature decreases below 0°C, and the fact that air is saturated over ice at temperatures less than about −15°C, 3) few actual reports of relative humidity above 96% due to the overcorrection of RH by the algorithm implemented in 1980 (Liu et al. 1991; Garand et al. 1992), 4) uncertainties in the RAOBS measurement discussed below, and 5) the effects of interpolation on some RAOBS with lower vertical resolution that may obscure the location of the cloud-layer edge (AWS 1979). The ΔT_d thresholds in our analysis are chosen based on the study in AWS (1979) that compared the behavior of RAOBS during cloud penetration with aircraft cloud-top and base observations. The reliability of the ΔT_d threshold is further tested by comparing its value at the cloud-base measured by surface observations.

Reporting humidity as a dewpoint temperature, derived from measured temperature and relative humidity, is the World Meteorological Organization standard practice. Errors in temperature and relative humidity values include random errors associated with poor instrument performance and systematic biases induced by instrument changes (Elliott and Gaffen 1991). Most contemporary rawinsonde instruments measure temperature and relative humidity with a precision of about 0.2°C and 3.5%, respectively. Performance becomes worse in cold and dry conditions. Elliott and Gaffen (1991) estimate random errors in the reported dewpoint values for U.S. rawinsondes by using the following equation:

$$E_{T_d} = \left[\frac{1}{T} - \frac{R_v}{L}\ln(U)\right]^{-2}\left[\frac{\Delta T}{T^2} + \left(\frac{\Delta U R_v}{LU}\right)\right], \quad (1)$$

where E_{Td} is error in dewpoint, T is temperature, R_v is gas constant for water vapor = 461 J (°C kg)$^{-1}$, U is relative humidity, L is latent heat of vaporization = 2.5×10^6 J kg^{-1}, ΔT is error of temperature, and ΔU is error of relative humidity. They find that errors in the reported T_d are <1°C for relative humidities >50% and temperatures >−20°C [see Fig. 1 in Elliott and Gaffen (1991)]. For 0.2°C and 10% errors in temperature and relative humidity for temperatures between −20° and −40°C, errors in the dewpoint temperature from Eq. (1) are still <2.5°C for relative humidities >50%. Therefore, at higher relative humidities where clouds form, the random errors in ΔT_d are 1–3°C, smaller than our thresholds.

Rawinsonde instruments have changed during the period covered by our dataset (1975–1988). Elliott and Gaffen (1991) show that the major changes in U.S. humidity-measuring systems in the period 1975–1988 were introductions of a new hygristor in 1980 and a complicated procedure for processing rawinsonde signals around 1980. These changes may have an impact on the humidity data, but at this time their overall effects are not clear and no equivalent information is available for rawinsondes in other countries. A rough estimate of the magnitude of any systematic errors induced by instrument and analysis method changes is that it is no larger than the random errors in the older measurements, since no large systematic shift in the relative humidities appears at the times of the changes (Gaffen et al. 1991). Thus, systematic changes in dewpoint temperature are probably no larger than 1–3°C for relative humidities >50%, smaller than our thresholds.

One year (1985) of data for station 723530 (Oklahoma City) has been examined in detail to determine the reasons for discarded RAOBS cloud layers, including mismatched or unmatched layers, and the frequency of occurrence of each situation. Table 2 gives the number of good cases (no problems at all) and lists all the types of problem cases from the total number of RAOBS and SWOBS reports available. The most frequent problem situations are 1) a SWOBS report of scattered cloudiness unmatched by a RAOBS moist layer (Type 1), presumably because the rawinsonde misses the scattered clouds; 2) multiple moist-layer situations where the extra layers in the same height category are eliminated (Type 7, but a cloud layer is retained so that these cases are eventually counted as good) or the SWOBS view of upper layers is obscured (Type 8, but the matched lower-level cloud is retained); 3) RAOBS moist layers reported as clear by SWOBS (Type 11, includes a few cases of bad SWOBS data); and 4) unexplained mismatches (Type 12). About 12% of possible cloud layers are discarded because of limitations of the two observing systems: missed higher moist layers with tops higher than the maximum altitude of the rawinsonde (Type 4 and Type 5) and frequently missed upper-level clouds by surface observers at night (Type 9). In about 10% of the cases, both datasets report a cloud layer but disagree on the height category (Type 12). Although no reason for this disagreement is apparent, we suspect that the surface observer's height estimate may be in error. Type 3 is also retained in the dataset with base heights obtained from the surface observer estimate. Although rejected in this analysis, most of the discarded cloud layers are probably real clouds, particularly Types 2, 4, 5, and 9 (about 13% of the total). Notably, rejected layers in

TABLE 2. Frequency of retained and discarded possible cloud layers and the reasons for discarding some observations.

Classification	Number/Fraction (%)	Explanation
Total	1513	
Total (cloudy layers)	644/43	Total cloudy (moist) layers are the sum of cloudy layers from "no problem" observations and Types 3, 7, and 8
"No problem"	495/33	
Cloudy	354/24	
Clear	141/9	
"Problem"	1018/67	
Type 1	186/12	RAOBS-missed scattered cloud layer reported by SWOBS
Type 2	20/1	Surface moist layer in RAOBS without fog or precipitation reported by SWOBS
Type 3	9/<1	Surface moist layer in RAOBS with fog or precipitation reported by SWOBS
Type 4	52/3	Moist layer extends above highest layer reported by RAOBS
Type 5	92/6	SWOBS-reported height of high cloud layer is above or close to last RAOBS reported height
Type 6	84/6	RAOBS cloud layer too thin: moist layer <100 ft (31 m) in low-height category and <200 ft (61 m) in mid- and high-height categories
Type 7	142/9	Duplicate RAOBS layer discarded: more than one moist layer in a height class, best match to SWOBS retained
Type 8	139/9	SWOBS view of RAOBS cloud layer blocked by overcast lower cloud layer
Type 9	35/2	Middle or high RAOBS cloud missed by SWOBS at night
Type 10	7/<1	Either RAOBS or SWOBS data missing
Type 11	108/7	RAOBS moist layer unmatched by SWOBS cloud, incomplete or miscoded SWOBS
Type 12	144/10	Unknown reason for mismatched layers

these cases have the effect of underestimating the occurrence of multiple cloud layers (see section 3c). Another 6% of the cases, included mostly in Type 11, have a RAOBS moist layer where SWOBS reports clear conditions. We discuss some possible improvements of the analysis method in the next section.

There are also sampling problems with the RAOBS that may cause biases in the cloud-layer statistics. Since RAOBS are more likely to penetrate broken and overcast clouds more often than scattered clouds, the climatology may underrepresent scattered cloud layers, which may have slightly lower tops and smaller layer thicknesses. The sampling of taller cumulus (Cu) and cumulonimbus (Cb) may be limited because they are generally scattered or small scale (we return to the issue of cloud-type sampling in section 3) or profiles may not reach their tops (Type 4). Moreover, such rapidly evolving clouds are not necessarily at vapor equilibrium owing to complications such as melting of snow or hail and entrainment of dry environmental air. Another problem is the thermal lag time of the rawinsonde humidity sensors that leads to lower than actual humidity reports whenever temperature decreases rapidly with altitude, so that both top and base heights AGL may be slightly too high. Moreover, this effect, together with finite vertical resolution, may cause thinner cloud layers to be missed (Type 6). The linear interpolation of temperatures may also cause errors in cloud-top and base heights. The top limit of RAOBS profiles (Types 4 and 5) eliminates some very high cloud layers or clouds that are thick enough to extend above 35 000 ft.

d. Possible improvements in analysis method

Many of the limitations in the observations eliminate real cloud layers when complete information and strict agreement between RAOBS and SWOBS are required, causing an underrepresentation of some cloud types in the climatology and an underestimation of the frequency of multilayered clouds (see Fig. 3). If the RAOBS were used alone with some restrictions relaxed, then more cases would be included even though the information would be incomplete in some cases.

Eleven percent of the cases (Type 8 and 9 in Table 2) are upper-level moist layers detected by RAOBS but not confirmed by SWOBS, either because that level is obscured by lower-level overcast or because the reliability of the surface observation is low at night. Had

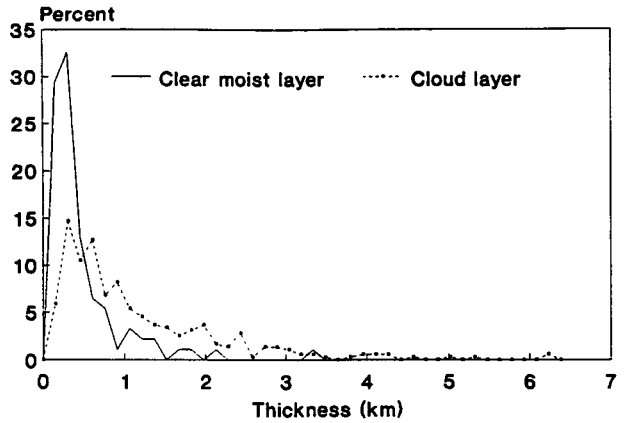

FIG. 1. Frequency distribution of layer thicknesses, Oklahoma City in 1985. Solid line is for clear moist layer, dotted line is for confirmed cloud layer.

the RAOBS been used alone, these multilayer cases would have been included. In addition, the cases where the RAOBS been used alone, these multilayer cases would have been included. In addition, the cases where the RAOBS detects more than one moist layer in the same height category would increase the total number of cloud layers by another 9% (Type 7 in Table 2). Both of these cases contribute to the dataset when the lower cloud layer is matched by the SWOBS report.

About 6% of the RAOBS detections are rejected because the layer thickness is too small (Type 6 in Table 2). The validity of this approach is reinforced by the detailed analysis of the Oklahoma City data that shows that about 6% of the total cases (mostly in Type 11 in Table 2), where the RAOBS detects a moist layer, are reported as clear by SWOBS. While 75% of these clear moist layers are thinner than 1500 ft (457 m), only 31% of the confirmed cloud layers are so thin (Fig. 1). These generally narrow layers may represent intrusions of moist air with very small or weak downward vertical motions so that no clouds actually form; whereas the cloudy cases may represent the same situation with small upward motions present or weak turbulence. Such cases may be biased by the rawinsonde's coarse vertical resolution and slow response time, both of which may underestimate the thickness of some cloud layers. Selecting the proper thickness criterion to distinguish between these cases will require more comparisons with surface and satellite observations.

Table 2 also shows that clouds with indeterminate bases, obscured by fog or precipitation or embedded in a very humid boundary layer (Types 2 and 3), constitute <2% of the cases. The number of cases, even in Oklahoma, with cloud-tops above 35 000 ft (Types 4 and 5) represent almost another 10% of the total. Both of these cases could be included either as incomplete reports or with cloud-base or cloud-top height estimated. Type 3 is included in the climatology where its base height AGL is taken from SWOBS.

Thus, if we add back all the cases that appear to be proper detections of cloud by the RAOBS (Types 2, 3, 4, 5, 7, 8, 9, and 11), we would have 63% of the total dataset reporting clouds, of which about 6% would be spurious detections (92 of Type 11). Also, 21% of the observations (Type 1 and clear cases) would be classified as clear, but more than half of these (Type 1) may be missed scattered clouds. Only 7% of the data (Type 6 and 10) would be classified as bad observations. The spurious detections only partially offset the missed scattered clouds; however, these thin moist layers are probably similar in thickness to the layers producing scattered cloudiness.

e. Climatology dataset description and availability

The cloud layer-thickness climatology (CLTC) dataset contains the individual RAOBS and SWOBS results for 14 years (1975–1988) for 63 sites in the Northern Hemisphere, a total of 210 227 observations. The geographic distribution of sites is shown in Fig. 2. Each observation reports layer-cloud amount, morphological type, high, middle, and low height class, top height AGL, base height AGL, and layer thickness, together with maximum RAOBS height used and station elevation. Henceforth, we will discuss only heights in meters above mean sea level using station elevation. Tables 1 and 3 describe the cloud-type codes and the arrangement and format of reported variables, respectively. The day/night flag is not correctly set for some stations, and for most stations it does not take seasonal variations into account. Appendix A lists the detail characteristics of the 63 sites. The CLTC dataset is archived at the National Center for Atmospheric Research.

3. Dataset characteristics and limitations

a. Geographic coverage

The geographic distribution of the 63 sites, shown in Fig. 2, samples Northern Hemispheric land areas

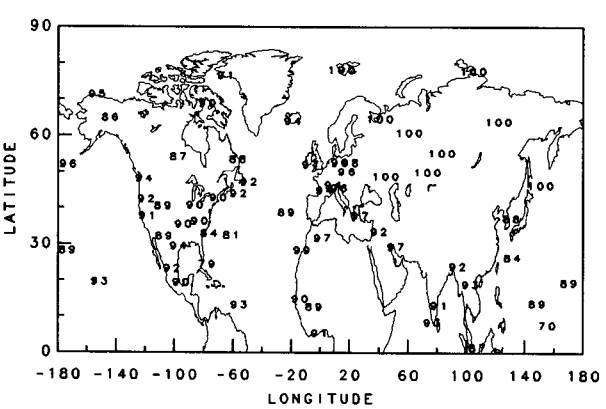

FIG. 2. Map of annual mean frequency of occurrence of one-layer clouds in percent for 1975–1988. This figure also shows the geographic distribution of the 63 RAOBS sites.

TABLE 3. Cloud layer record format.

Columns	Name	Explanation
1–6	Station	Block station number (039530-913340)
8–9	Year	Year
11–12	Month	Month (1–12)
14–15	Day	Day (1–31)
17–18	Hour	Hour (00 or 12), UTC
21–25	Latitude	In degrees and minutes, DD.MM
27–33	Longitude	Degrees and minutes, DDDD.MM, negative is east
35–39	Elevation	Station elevation in feet
41–45	Day/Night	Day or night flag, see note below
47–51	Max Height	Maximum RAOB height used, in feet AGL
53	Height Class	Height class flag, 1 = low (base < =6500 ft), 2 = middle (base 6501–16 500 ft), 3 = high (base > 16 500 ft)
55	Amount	Cloud amount, in eighths, from the surface observation, missing data is indicated by a period (.)
57–58	Type	Layer type (see Table 1)
60–64	Base	Cloud base in feet AGL
66–70	Top	Cloud top in feet AGL
72–76	Thickness	Thickness in feet

Note: The day/night flag was originally designed to help look for diurnal cloud-height variation and determine whether cloud layers were accurately analyzed. It is not correctly set for some stations, and for most stations it does not take seasonal variation into account. You should not use this variable unless you validate it for a particular station.

reasonably well, except for some land types such as the Sahara Desert and the major monsoon regions (India and southern Asia). Island sites and near-coastal sites are used to represent ocean areas, but large portions of the oceans, particularly in the Tropics, are not covered. Moreover, these sites may not actually represent the marine environment accurately. There are some long observation records from the permanently stationed weather ships, but these have not been analyzed. There are no stations in the polar regions (80°–90°N). Because of the sparse site coverage, we cannot use the dataset to produce a regional or local climatology. We concentrate on zonal averages but separate them into land and ocean subsets.

b. *Temporal coverage*

Table 4 shows the distribution of observations by latitude zone and season and indicates that the sampling is relatively uniform over all seasons in each 10° latitude zone (Northern Hemisphere). The seasonal variations of the number of observations at individual sites may indicate that some are not suitable for analyzing seasonal variations of cloud properties; however, since the dataset contains only cloudy reports, some of this seasonal variation of observation number is associated with variation of the frequency of cloud occurrence.

TABLE 4. Number of observations.

Latitude (°N)	December–February	March–May	June–August	September–November
0–10	2131	2181	2975	2780
10–20	6209	6961	9942	8359
20–30	4612	4703	5269	4971
30–40	9377	9486	9335	8998
40–50	12969	12062	9327	11579
50–60	8984	8836	8887	9817
60–70	3121	4189	5582	4896
70–80	1398	2395	4749	3147

Since only two observations per day are used from each site (0000 and 1200 UTC), diurnal variations at individual sites cannot be determined. Although observations are well distributed over different diurnal phases within each 10° latitude zone, the combined results cannot be used to study diurnal variations because they also include systematic longitudinal variations. Diurnal variations could be studied in some regions, such as Europe, where many stations collect RAOBS four times per day. [This has been done at many sites in the United States before 1957 (Schwartz and Doswell 1991)].

c. *Cloud-layer overlap statistics*

The frequency of occurrence of single-layer clouds in the dataset is shown in Fig. 3. Over most sites the frequency of single-layer clouds is ≥90%; but over the nine Russian sites all clouds are reported as single layer. Tian and Curry (1989) analyzed the vertical distribution of clouds during January 1979 over the North Atlantic Ocean (40°–60°N) and found that 63% of the cloudy cases are composed of one layer, while the nearest site (No. 039530) in the CLTC dataset has a 97% frequency of single-layer clouds. Using the co-occurrence frequencies of clouds from a climatology

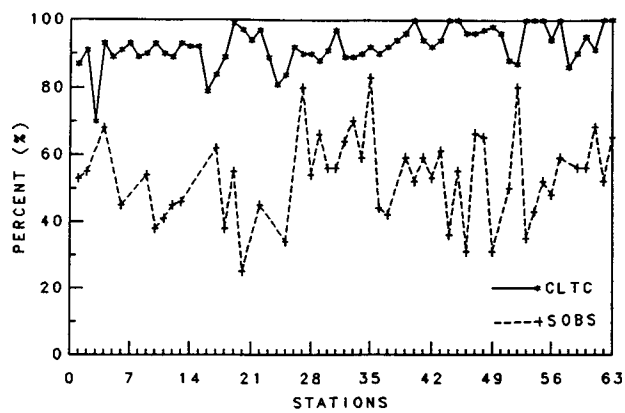

FIG. 3. Comparison of annual mean frequencies of occurrence of one-layer clouds over the 63 sites from the CLTC for 1975–1988 and from SOBS for 1971–1981 (Warren et al. 1986; Warren et al. 1988).

of surface observations (SOBS) (Hahn et al. 1982, 1984), we estimate the frequency of one-layer clouds and compare it with this dataset (Fig. 3). The CLTC dataset underestimates the frequency of multilayer clouds, which is attributed to the underrepresentation of middle and high clouds in the CLTC discussed in section 2c and in the next section. On the other hand, SOBS might overestimate high clouds and, consequently, cause higher frequency of occurrence of multilayered clouds because the probability of an upper cloud, given a lower cloud, is assumed to be the same when high cloud cannot be seen (because low cloud is overcast) as when it can be seen (when low cloud is present but not overcast) (Hahn et al. 1982, Warren et al. 1985). The possible improvements in analysis method mentioned in section 2d would increase the frequency of occurrence of multilayer clouds in the RAOBS dataset.

d. Sampling effects

We further evaluate the sampling of the CLTC dataset by comparing cloud cover fractions, frequencies of occurrence of cloud types, and base heights AGL of low clouds (cumulus = Cu, stratus = St, and cumulonimbus = Cb) with SOBS (Hahn et al. 1982, 1984; Warren et al. 1986, 1988). For the comparisons, the 10 cloud types in the CLTC dataset are grouped into six categories (Table 1), which is the same classification adapted by Hahn et al. (1982, 1984); Warren et al. (1986) and Warren et al. (1988). The average value of each cloud quantity (cover, frequency of occurrence, and base height) for six types of clouds from CLTC and SOBS are considered to have 63 observations to calculate correlation coefficients. All correlation coefficients are above the 99% confidence level, except for nimbostratus (Nb) clouds (Table 5). Figure 4 shows the comparison of the frequency of occurrence and cloud cover fraction for St clouds over the 63 sites from our dataset and from SOBS: they vary together over the 63 sites with a small positive systematic difference (CLTC > SOBS) in magnitude at higher latitudes (larger station numbers). Similar results are found for cirrus (Ci) and nimbostratus (Ns) with a similar but negative systematic difference at higher latitudes. Apparently the CLTC undersamples Ci and Ns clouds and oversamples St clouds at middle to high latitudes. Undersampling of Ci and Ns and the underestimate

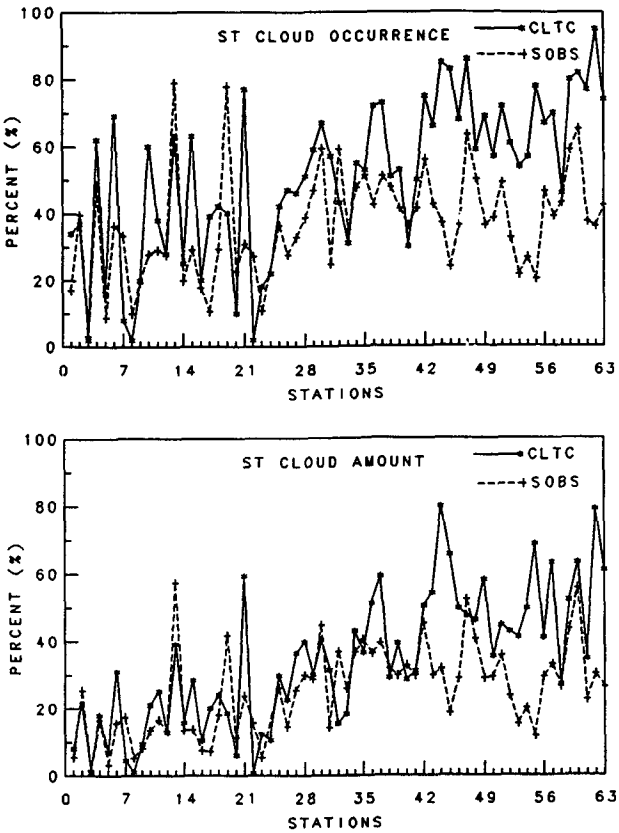

FIG. 4. Comparison of annual mean frequencies of (a) occurrence of stratus clouds and the (b) stratus cloud amounts over the 63 sites from the CLTC for 1975–1988 (solid lines) and from SOBS for 1971–1981 (dotted lines) (Warren et al. 1986; Warren et al. 1988).

TABLE 5. Comparisons of cloud amount and frequency of occurrence of six types of cloud and cloud-base heights of Cu, St, and Cb from CLTC and SOBS.

Type	Ci	As	Ns	Cu	St	Cb
Frequency						
Correlation coefficients	0.50	0.43	0.23	0.67	0.53	0.83
Rms difference (%)	13	12	7	13	24	6
Average difference (%)	−10	−1	−5	2	14	0
Amount						
Correlation coefficients	0.60	0.32	0.28	0.57	0.56	0.89
Rms difference (%)	5	8	7	5	18	5
Average difference (%)	−3	1	−5	1	8	0
Base height						
Correlation coefficients	—	—	—	0.15	−0.06	0.05
rms difference (m)	—	—	—	391	411	398
Average difference (m)	—	—	—	−103	−146	−66

of multilayer clouds mentioned above are consistent with the conclusion drawn in section 2c. Mean annual base heights AGL of St over the 63 sites from CLTC and SOBS are shown in Fig. 5. There are similar results for Cu and Cb (not shown). The general agreement in magnitude is good (Table 5, average differences are less than 150 m), except at a few sites, but the correlation of the two datasets is negligible (Table 5). This low correlation may be due to the different years covered by the two datasets, together with the effects of sampling in the CLTC. The root-mean-square (rms) differences can be used as one estimate of the uncertainties: for all three cloud types, the rms differences of mean base heights AGL from two datasets are about 400 m, which is similar to the standard deviation of mean base heights AGL from CLTC, 430 m, suggesting that the variations of low cloud-base heights are dominated by measurement uncertainty.

The top heights above mean sea level (MSL) of the highest clouds in each CLTC profile have been compared with satellite measurements from ISCCP (Rossow and Schiffer 1991). Average top heights from all 63 sites are collocated with individual map grid cells of multiyear monthly mean values derived from ISCCP cloud-top pressures using a standard atmospheric profile. Spatial and seasonal variations in cloud-top heights from the two datasets have a correlation coefficient of 0.54, but the CLTC values are about 1211 m smaller than the ISCCP values. The detailed variations of the differences with climate regime (cloud type) suggest that the primary cause of this difference is the undersampling of middle- and high-level clouds in CLTC, as discussed in section 2. More detailed comparisons are warranted; however, this comparison provides an upper limit to the average errors in the CLTC cloud-layer heights. In this study we focus on the cloud-layer thickness information provided by CLTC.

To test whether results from the 63 sites form meaningful zonal averages, we also compared the latitudinal and seasonal variations of zonal-mean cloud-cover fraction, cloud-top altitude, and optical thickness over land and ocean from ISCCP data using all map grid cells at each latitude with the zonal-mean values calculated using only the 63 grid cells where the RAOBS sites are located. Although there are quantitative differences caused by the small sample, the overall latitudinal variation of cloud properties is captured; however, seasonal variations at higher latitudes are not well represented. An ongoing study of a rawinsonde collection over 36 ocean sites (11 weather ships and 25 islands) will test whether the ocean results in the current dataset (islands and coastal sites) are representative.

We also note that, since only two observations per day (0000 and 1200 UTC) are used in the CLTC dataset, there is the possibility that our zonal averages are biased by the limited diurnal sampling, even though the distribution of diurnal phases associated with the longitude variations of the sites is relatively uniform.

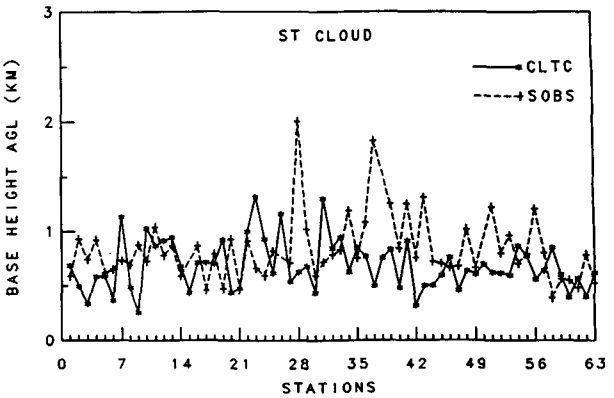

FIG. 5. Comparison of annual mean cloud base altitudes for stratus clouds over the 63 sites from the CLTC for 1975–1988 (solid lines) and from SOBS for 1971–1981 (dotted lines) (Warren et al. 1986; Warren et al. 1988).

e. Cloud classification

One way to summarize our results is to present average results for different cloud types; however, there are several possible schemes for classifying clouds. The traditional cloud type names are primarily morphological but are interpreted in terms of height above ground level. Such a classification actually mixes clouds at different heights because of the variation of surface topography. Figure 6 shows the distribution of cloud-base and cloud-top heights MSL (altitudes) and layer thicknesses sorted by the matching surface observer's morphological identification (Table 1). Two low-level cloud types, Cu and St, exhibit very similar property distributions, whereas another low-level cloud type, Cb (classified as low level because of base height), is very different. The Ns type clearly includes a very wide range of cloud properties, whereas altostratus has a narrower range of properties. Satellites, on the other hand, classify clouds more naturally by cloud-top height; Fig. 7 shows the distribution of cloud-layer properties for high-level clouds. The mixture of thicker- and thinner-layer clouds (with different base heights) changes with latitude, as shown, and with season (not shown).

An examination of the layer thickness frequency distributions for individual sites, mostly in Russia, shows that some stations at high latitudes are characterized by unimodal distributions of unusually thick clouds, which is the main contributor of higher frequency of thicker clouds at high latitudes (Fig. 7). These sites also report frequencies of occurrence of Cb that are 2–5 times higher than in the full SOBS cloud climatology, which is partly due to the practice of reporting nearly all cumuliform clouds as Cb instead of cumulus and stratocumulus. This practice, however, may also enhance the sampling of such cases in the climatology because the required agreement between SWOBS and RAOBS results in higher sampling of Cb clouds that are very thick. Cumulonimbus cloud may

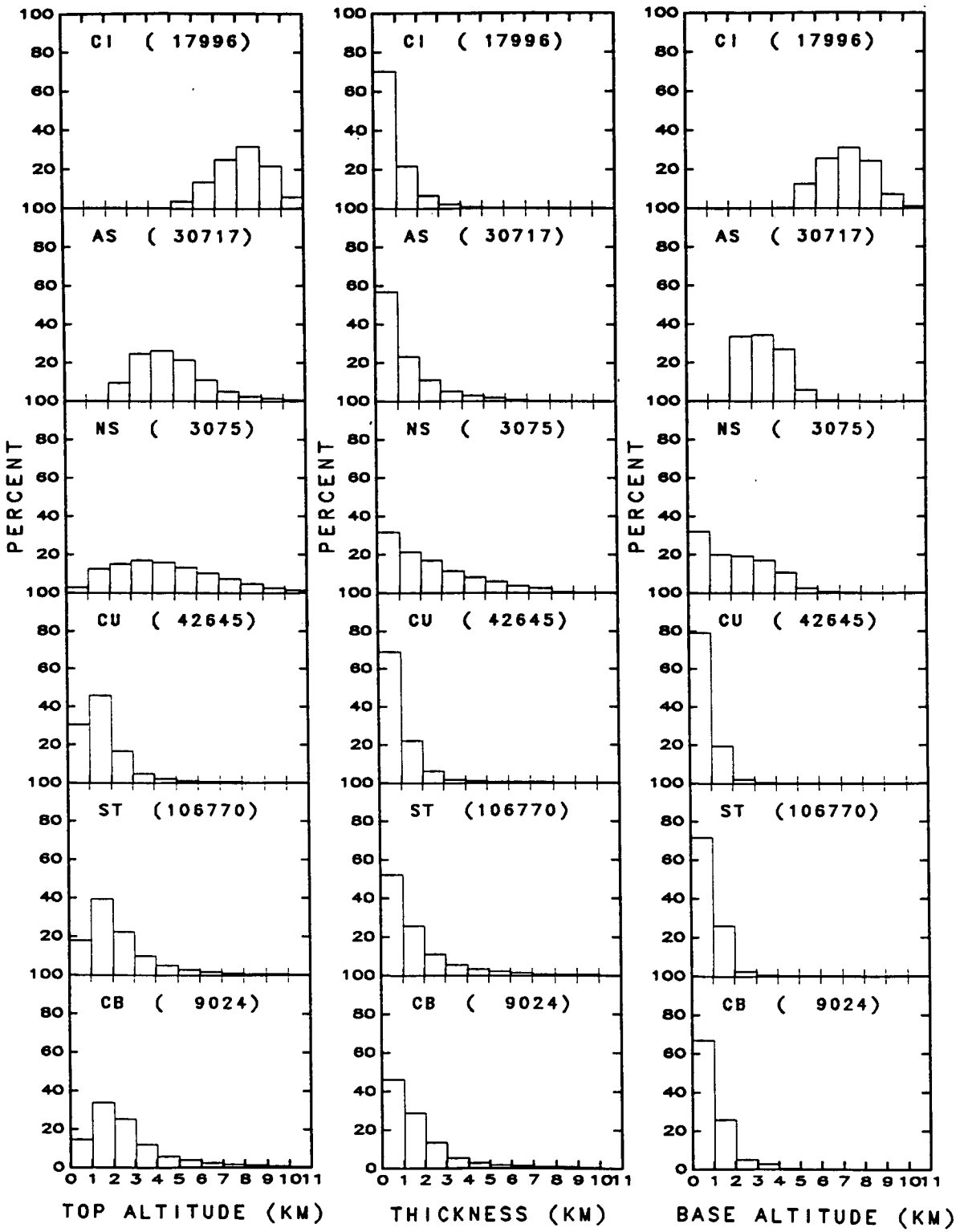

FIG. 6. Frequency distributions of cloud-top altitude, layer thickness, and base altitude for the six cloud types defined in Table 1. The numbers in parentheses are the number of observations.

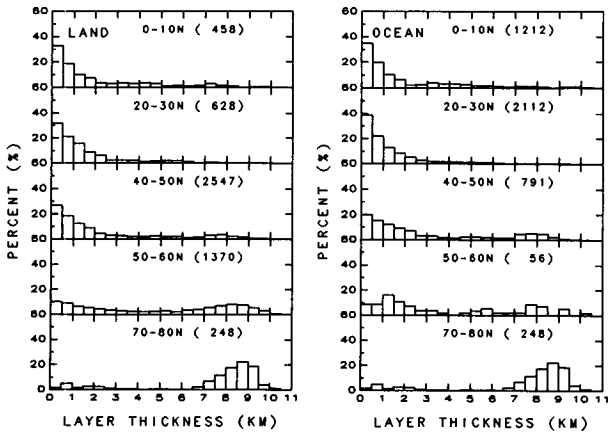

FIG. 7. Frequency distributions of layer thicknesses for high-top clouds (altitudes = 7600–11 000 m) (a) over land and (b) over ocean in 10° latitude zones. The numbers in parentheses are the number of observations.

also obscure many high and thin clouds from surface observation.

4. Results

a. Global statistics

We collected the statistics of cloud layer thicknesses (Δz) using two altitude classifications (referred to as "high/mid-/low-top" or "high/mid-/low base" clouds), as well as the six morphological cloud types. Low, middle, and high clouds are defined by base altitudes $z_b \leq 2000$ m, $2000 < z_b \leq 5000$ m, and $z_b > 5000$ m, respectively, or by top altitudes $z_t \leq 3000$ m, $3000 < z_t \leq 7600$ m, and $z_t > 7600$ m (up to about 10 700 m), respectively. In the results shown, heights are MSL. For each 10° latitude zone and season, we collected statistics for land areas (34 inland and 14 coastal sites) and for ocean areas (15 island and 14 coastal sites). The 14 coastal sites (22% of the total) have been used twice.

The frequency distributions of cloud-base altitude, layer thickness, and top altitude in 0°–20°N, 20°–40°N, and 40°–80°N zones without any classification are shown in Fig. 8. Most clouds have layer thicknesses between 0 and 3000 m with an average of 1262 m, but there is a slightly higher frequency of thicker clouds at higher latitudes (Fig. 8b). Cloud-top altitudes exhibit a wide range from 500 m to 10 000 m with an average of 3017 m, but most clouds tops are below 4000 m. The distribution of cloud-top altitudes is roughly similar at all latitudes, with somewhat more midlevel cloudiness at latitudes >40° and more cloud-tops above 9000 m in the Tropics (Fig. 8a). The latter feature is probably underestimated because of the height limits on RAOBS. Cloud-base altitudes are predominantly in the range 0–2000 m with an average of 1755 m, but there are two apparent secondary modes at 2000–5000 m and 5000–11 000 m in the Tropics (Fig. 8c). These tropical cloud-base altitude modes are associated with the classification by base heights AGL in the dataset and may be exaggerated by the required agreement between RAOBS and SWOBS base-height estimates.

Table 6 summarizes mean cloud-top and cloud-base altitudes and cloud-layer thicknesses for all three types of classification, both over land and over ocean. Average cloud-base and cloud-top altitudes are similar for clouds classified by either base or top altitudes; however, layer thickness variations change with classification. If clouds are grouped by base altitudes (as surface observers do), then average cloud-layer thicknesses decrease from low to high clouds. If clouds are grouped by top altitudes (as satellites do), then layer thicknesses increase from low to high clouds. Of the morphological types, Ci have the smallest layer thicknesses and Nb have the largest. The surprisingly small

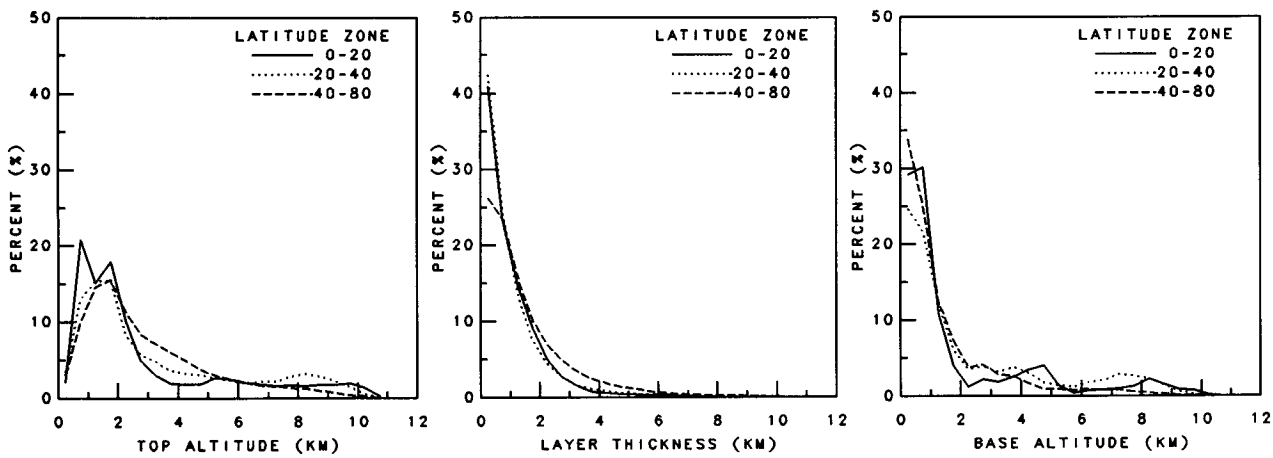

FIG. 8. Frequency distributions of cloud-top altitudes, layer thicknesses, and base altitudes for all 210 227 observations in three latitude zones: 0–20°N, 20°–40°N, and 40°–80°N.

layer thickness for Cb clouds is probably an artifact produced by mixing nonprecipitating but vertically developed cumulus with precipitating storm clouds in the surface classification, and by the altitude limits of the RAOBS.

b. *Zonal and seasonal variations*

Figure 9 shows that, without any classification, both average cloud-top and base altitudes decrease with latitude over land and ocean. The values in the 10°–20°N zone over land are exaggerated by a maximum in mean station elevation, however. Cloud layer thicknesses vary little with latitude or between land and ocean. When clouds are classified by base altitudes, the zonal average variations of layer thicknesses are negligible. Zonal average variations of layer thicknesses are more marked when the clouds are classified by cloud-top altitudes (Fig. 10). There are three remarkable features: 1) the mean layer thickness of low-top clouds is about 1000 m at all latitudes, 2) the layer thickness of midtop and high-top clouds increases with latitude, especially for high-top clouds, and 3) a minimum of layer thickness for high-top clouds occurs in the 20°–30°N zone over land and in the 30°–40°N zone over ocean.

Seasonal variations of layer thicknesses and base and top altitudes without any classification show that clouds over tropical land are thickest and have their lowest bases in summer, while at middle and high latitudes over land and at all latitudes over ocean, seasonal variations of layer thicknesses are insignificant. Cloud-base altitudes exhibit a small increase in summer at middle and high latitudes, particularly over land. Cloud-top altitudes have the same seasonal variation pattern as base altitudes, but with smaller magnitude. When clouds are classified by base altitudes, there is no significant seasonal variation of cloud-layer thicknesses; but when clouds are classified by top altitude, noticeable seasonal variations of cloud-layer thickness occur for high-top clouds (Fig. 11). Over land, high-top cloud layer thicknesses reach a summer maximum in the Tropics, a weak summer minimum in the subtropics, and a strong summer minimum at higher latitudes (Fig. 11a). The same features exist over ocean,

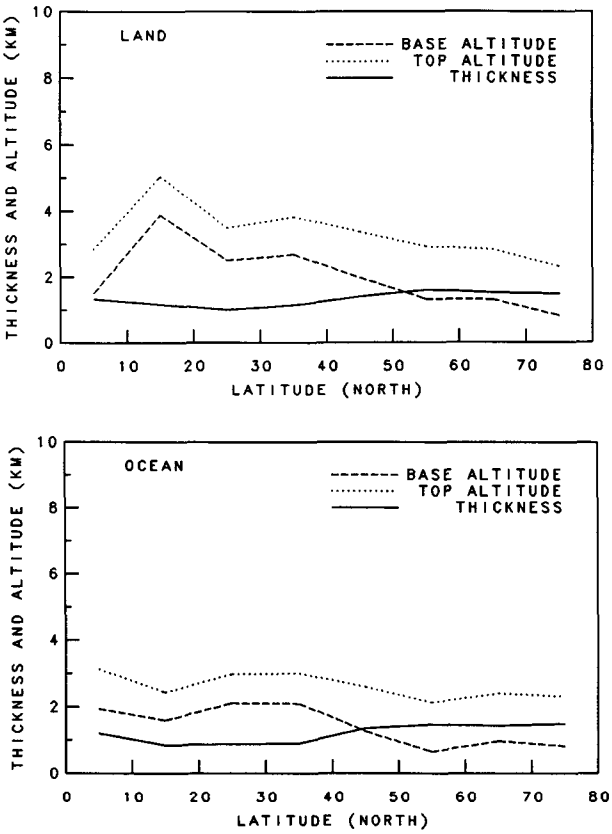

FIG. 9. Latitude variations of average cloud-top and base altitudes and layer thickness for all 210 227 observations over (a) land and (b) over ocean.

TABLE 6. Cloud-top altitude, layer thickness, and base altitude (in m).

	Land			Ocean		
	Top	Base	Thickness	Top	Base	Thickness
Mean	3203	1799	1384	2640	1532	1097
Low top	1620	773	858	1441	657	795
Midtop	4768	2671	2091	4893	2820	2083
High top	8733	6254	2484	8834	7097	1740
Low base	2210	729	1480	1721	616	1111
Midbase	4623	3305	1321	4683	3396	1285
High base	7858	6994	865	8190	7374	817
Ci	8101	7252	848	8235	7423	811
As	4831	3577	1250	4673	3437	1235
Ns	4509	2094	2414	4098	1950	2147
Cu	2076	920	1158	1391	592	799
St	2282	758	1518	1891	623	1263
Cb	2895	1145	1794	1957	618	1338

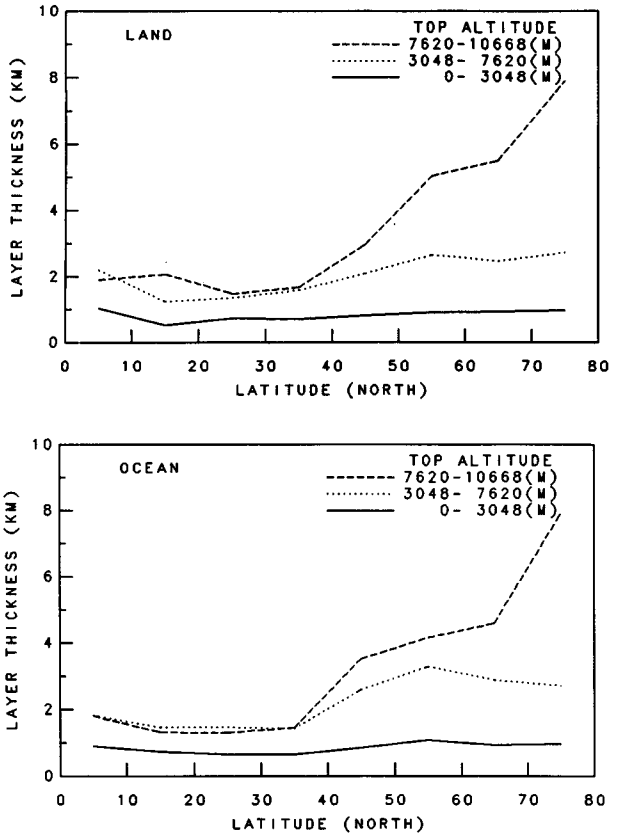

FIG. 10. Latitude variations of average cloud layer thicknesses (a) over land and (b) over ocean for high, middle, and low clouds defined by top altitudes.

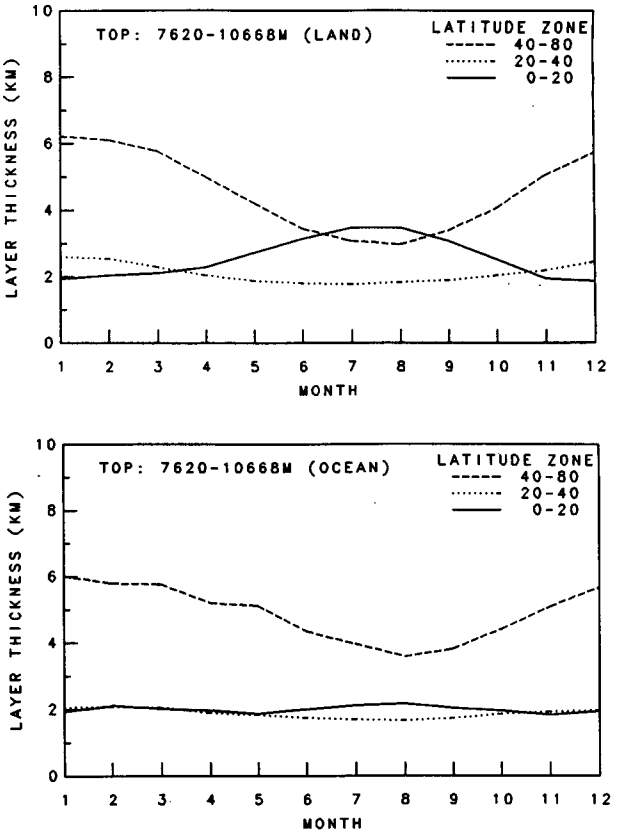

FIG. 11. Seasonal variations of high-top cloud layer thicknesses (a) over land and (b) over ocean in three latitude zones: 0°–20°N, 20°–40°N, and 40°–80°N.

but with much smaller magnitudes (Fig. 11b). Midtop clouds show only slight seasonal variations at lower latitudes whereas low-top clouds show no variations.

The thickness of the clear surface layer is defined by the base height AGL of the lowest cloud. Clear surface-layer thickness decreases with latitude, particularly over land, and has a maximum in the 10°–20°N zone over land and in the 20°–30°N zone over ocean. The maximum over land moves from 10°–20°N in winter to 30°–40°N in summer. Seasonal variations of the clear surface-layer thicknesses for different latitudinal zones over land (Fig. 12) show that the clear surface-layer thickness reaches a summer minimum in the Tropics and a summer maximum in the subtropics and middle latitudes. There is no significant seasonal variation of clear surface-layer thicknesses over ocean, although there is a suggestion of a summertime increase at higher latitudes.

To test whether latitudinal variations in average cloud-layer thickness shown in Figs. 9 and 10 are significant in comparison to sampling errors, we calculated standard deviations of individual observations of cloud-layer thicknesses in each 10° latitude zone for all low-top, mid-top, and high-top clouds. According to the central limit theorem, the standard deviations of average layer thicknesses in each 10° latitude zone can be approximately estimated as the standard deviations of individual observations divided by the square root of the number of observations. Such standard deviations are estimates of sampling errors in average layer thicknesses.

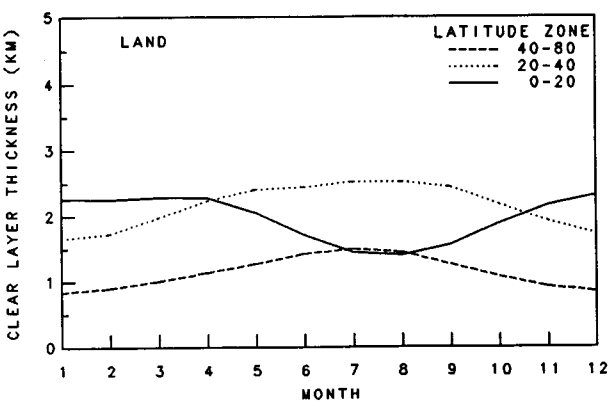

FIG. 12. Seasonal variations of average clear surface-layer thicknesses over land in three latitude zones: 0°–20°N, 20°–40°N, and 40°–80°N.

They exhibit minor latitudinal variations. Table 7 shows averaged sampling errors in eight latitude zones for all, low-top, midtop, and high-top clouds. The amplitude of strong latitudinal variations of high-top cloud-layer thickness shown in Fig. 10 is much larger than the sampling errors in Table 7 (95 m and 139 m over land and ocean, respectively). Likewise, sampling errors of average layer thicknesses in each month in 0°–20°N, 20°–40°N, and 40°–80°N zones shown in Fig. 11 are computed, and the averages over 12 months are also shown in Table 7. The seasonal variations of high-top cloud-layer thicknesses in the 0°–20°N zone over land and the 40°–80°N zone over land and ocean shown in Fig. 11 are significant because of much smaller sampling errors shown in Table 7. Similarly, the seasonal variations of average clear surface-layer thicknesses shown in Fig. 12 are also shown to be significant.

TABLE 7. The sampling errors (in m) averaged in eight latitude zones and averaged in 12 months in 0°–20°N, 20°–40°N, and 40°–80°N zones for all, low-top, midtop, and high-top clouds. The first number in each column is for land and the second for ocean.

	All	Low-top	Midtop	High-top
Averaged in 8 latitude zones	13/11	8/7	27/32	95/139
Averaged over 12 months				
0°–20°N	41/18	31/13	70/77	194/114
20°–40°N	24/18	16/12	49/56	102/89
40°–80°N	17/24	9/13	31/62	175/357

c. *Distribution of cloud properties by cloud morphological types*

The cloud-top altitudes, layer thicknesses, and base altitudes of the six morphological cloud types over land and ocean in Table 6 show four notable features: 1) the mean cloud-layer thickness ranges only from 800 m to 2400 m; 2) Cu clouds over ocean and Ci clouds have the smallest layer thicknesses; 3) Ns clouds have the largest layer thicknesses; and 4) Cloud layers for each type are thicker over land than over ocean. The layer thicknesses for Ci and altostratus clouds ($\sim$1000 m) are consistent with other results (Cotton and Anthes 1989). There are no significant zonal and seasonal variations of layer thicknesses for the six morphological cloud types. That the properties of individual cloud types are approximately constant, yet the high-top clouds, at least, exhibit significant latitudinal and seasonal variability suggests that these variations might be explained by changing mixtures of different cloud types.

d. *Relations among cloud-top altitude, layer thickness, and base altitude*

We examine the correlations among cloud-top altitude, layer thickness, and base altitude in separate latitude zones (0°–20°N, 20°–40°N, and 40°–80°N) by plotting the frequency distributions in three domains defined by z_b and z_t, Δz and z_t (Fig. 13), and Δz and z_b (not shown). In the first domain (Fig. 13a), there are three distinct peaks in the frequency distribution in the Tropics, a suggestion of a secondary peak in the subtropics, and no clear separation of the distribution apparent at higher latitudes (cf. Fig. 8). The same clusters appear along the cloud-top (or base) altitude axes with little separation of layer thicknesses (Fig. 13b). At higher latitudes, Fig. 13b shows two groups of clouds, one with layer thicknesses proportional to their cloud-top altitudes and one with a small ($\leq$1000 m) layer thickness independent of cloud-top altitude. Some suggestion of a proportionality between layer thickness and cloud-top altitude also appears in each of the groups at lower latitudes.

5. Discussion

In the absence of comprehensive measurements of cloud vertical distribution, we must exploit several partial descriptions obtained from surface observations, satellites, and RAOBS. RAOBS have not been used much before for this purpose. Despite the sparse geographic coverage and poor diurnal sampling of the current dataset, it provides a first glimpse of the large-scale variations of cloud-layer thicknesses from coincident measurements of cloud-base and cloud-top altitudes. Much more remains to be done to verify the accuracy of the measured cloud-base and cloud-top altitudes by comparison with surface (e.g., lidar, radar, and ceilometer) and satellite measurements, but initial comparisons indicate uncertainties less than 1000 m for low- and midlevel clouds. The largest drawback to the RAOBS measurements is their low sensitivity to upper-level moisture and clouds. In addition, the current analysis method, which requires strict agreement with surface observations, does not adequately represent multilayer cases. Even with these limitations, examination of these first results suggests some interesting conclusions that are listed below. We take these conclusions to be preliminary until the RAOBS analysis can be more thoroughly checked against other measurements and the number of sites increased to improve the geographic coverage.

(a) Most clouds and cloud types have layer thicknesses in the range 0–3000 m (Table 6, Fig. 6), but there exist some clouds with layer thicknesses up to 9000 m (Fig. 8). The layer-thickness distributions for all cloud types are roughly similar and very broad. These distributions suggest that even the morphological cloud types, which represent large changes in the dynamic regime (weather), do not explain the large-scale differences in cloud-layer thicknesses that we find. Other factors besides dynamics influence the layer thickness of individual examples of these cloud types, for example, the effects of surface fluxes of heat and moisture, direct radiative effects on the cloud

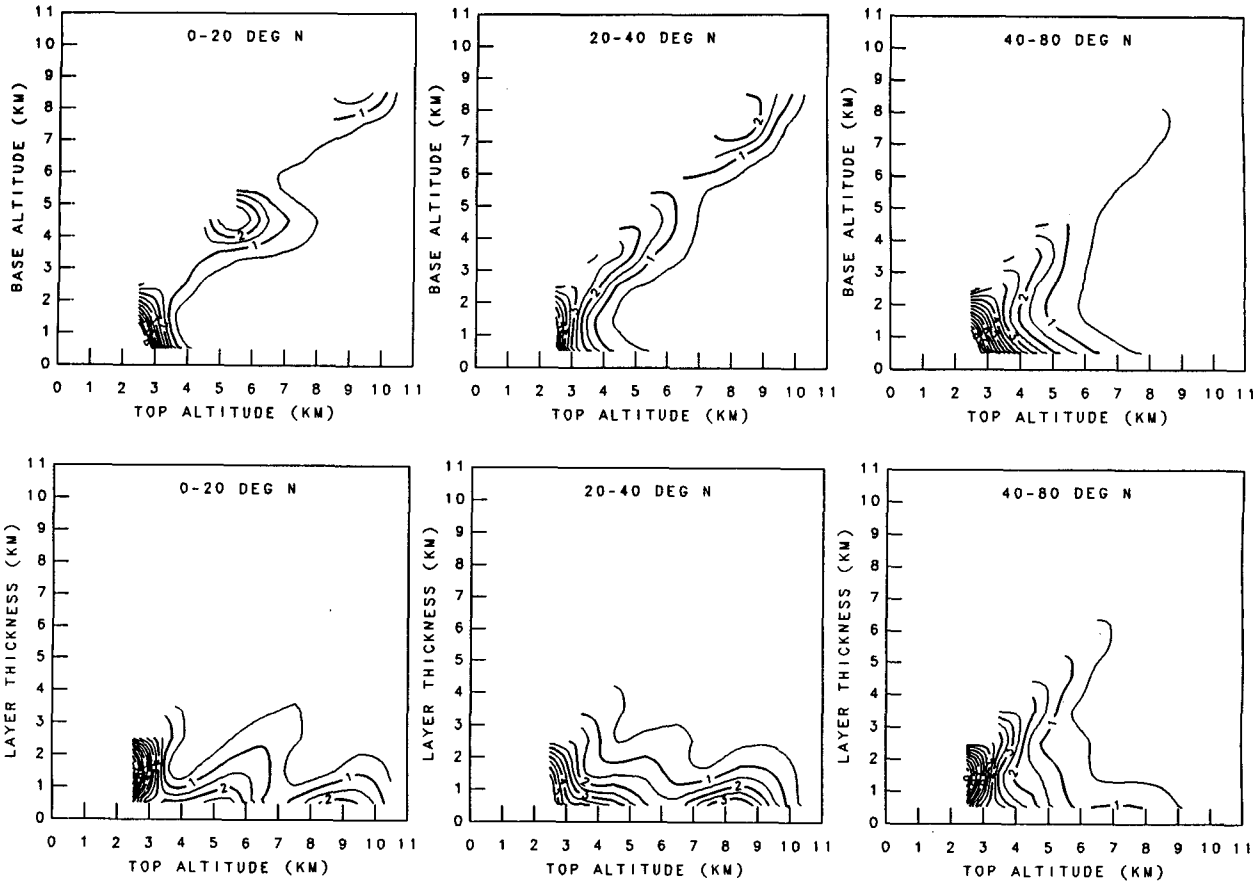

FIG. 13. Two-dimensional frequency distributions showing relationships (upper panels) between cloud-base altitude and top altitude and (lower panels) between cloud-layer thickness and top altitude in three latitude zones: 0°–20°N, 20°–40°N, and 40°–80°N. Contours indicate frequencies in percent relative to total number of observations.

dynamics, and other dynamical effects, such as cloud-top entrainment, which determines the thickness of boundary layer clouds (Betts 1989).

(b) When clouds are classified by top altitude, there are zonal and seasonal variations of their average layer thicknesses that appear to correspond to major features of the atmospheric general circulation. The minimum of cloud-layer thicknesses in the 20°–30°N zone over land coincides with the mean subsidence zone of the Hadley circulation. This region of minimum layer thickness moves southward to 10°–20°N in winter, which corresponds to the movement of the subsidence region. The occurrence of a summer maximum in high-top clouds over tropical land coincides with the seasonal motions of the intertropical convergence zone, which is associated with changes in the upwelling part of the Hadley circulation. The occurrence of thicker high-top clouds in the extratropics rather than in the Tropics, with the thickest high-top clouds occurring in winter, coincides with the zone of extratropical cyclonic storms and with a strengthening of those storms in winter.

The differences between the distributions of cloud-base and cloud-top altitudes in the Tropics and the extratropics (Fig. 13) indicate different cloud system organizations. Tropical clouds occur in cloud systems that are formed by small-scale convective processes and associated mesoscale circulations with strong vertical motions and distinct base altitudes (Air Ministry Meteorological Office 1956; Cotton and Anthes 1989). Extratropical clouds, on the other hand, are generally formed by large-scale lifting of moist air in association with cyclonic storms, and have more varied base altitudes (Cotton and Anthes 1989).

(c) Cloud vertical structure affects the vertical distribution of latent heating and radiative heating/cooling which, in turn, affects atmospheric dynamics. This interaction is one of the fundamental feedbacks in the climate system. Currently, we have little quantitative information about cloud vertical structure except the frequencies of occurrence of cloud-bases and cloud-tops, as well as cloud-type information. Our dataset can be used in combination with surface and satellite observations to improve the description of cloud vertical distributions that are used in the study of the interaction between cloud-radiative effects and atmospheric dynamics. For example, the combination of cloud-layer thickness for clouds clas-

sified by cloud-top altitudes (Fig. 14) and satellite-measured cloud-top altitudes can be used in calculations of surface radiative fluxes (Zhang et al. 1995). This method of inferring cloud-base height (AGL) can also be checked against the clear surface-layer thicknesses statistics that we obtain. Figure 12 shows that clear surface-layer thicknesses vary with season over land, particularly in the Tropics, but not over oceans. In addition, the base altitudes of middle and high clouds also vary with latitude and season.

(d) Our dataset can also be used to investigate the influences of cloud physical thickness on optical thickness. Cloud optical thicknesses of low-top clouds increase with latitude [see Figs. 2 and 3 in Tselioudis et al. (1992)]. We have found that the latitudinal and seasonal variations of the layer thicknesses of low-top clouds are negligible, which reinforces the interpretation of Tselioudis et al. (1992) that the observed variations in the optical thicknesses of low-top clouds represent changes in cloud-water content. On the other hand, high-top cloud layer thicknesses exhibit significant latitudinal and seasonal variations that must have substantial effects on their optical thicknesses (Platt and Harshvardhan 1988; Platt 1989) and may help explain more complicated variations of cirrus optical thicknesses (Tselioudis and Rossow 1994). A more complete study of the role of cloud physical thicknesses in changing cloud optical thicknesses can be done by combining our dataset with satellite observations to determine the systematic variations of physical and optical thickness with temperatures.

The CLTC dataset has six limitations: 1) no Southern Hemisphere information; 2) poor coverage over some types of land; 3) no coverage of the central parts of the oceans, particularly in the Tropics, and the polar regions; 4) no diurnal sampling; 5) under- or overrepresentation of some cloud types in the statistics; and 6) underrepresentation of multilayer cloud situations. We can improve the coverage over land by analyzing more data from land sites selected with particular attention to coverage of deserts and monsoon climates and improve the coverage over oceans by collecting more observations from other islands and adding weather ship observations. There are now available long-term RAOBS collected in Russia and at Russian ice islands in the Arctic that may be used to improve coverage of the North Polar region (Kahl et al. 1992). The limitation on diurnal sampling may be removed by collecting the other daily observations made at the sites already included and by using the extra data, such as the 0600 UTC or 1800 UTC RAOBS taken at some stations. The geographic coverage that can be obtained with adequate diurnal sampling is not known, however. Furthermore, off-hour and special study of RAOBS, such as those collected at Patrick and Vandenberg Air Force Bases for space launches, could be useful for studies that cover very broad areas or have very long

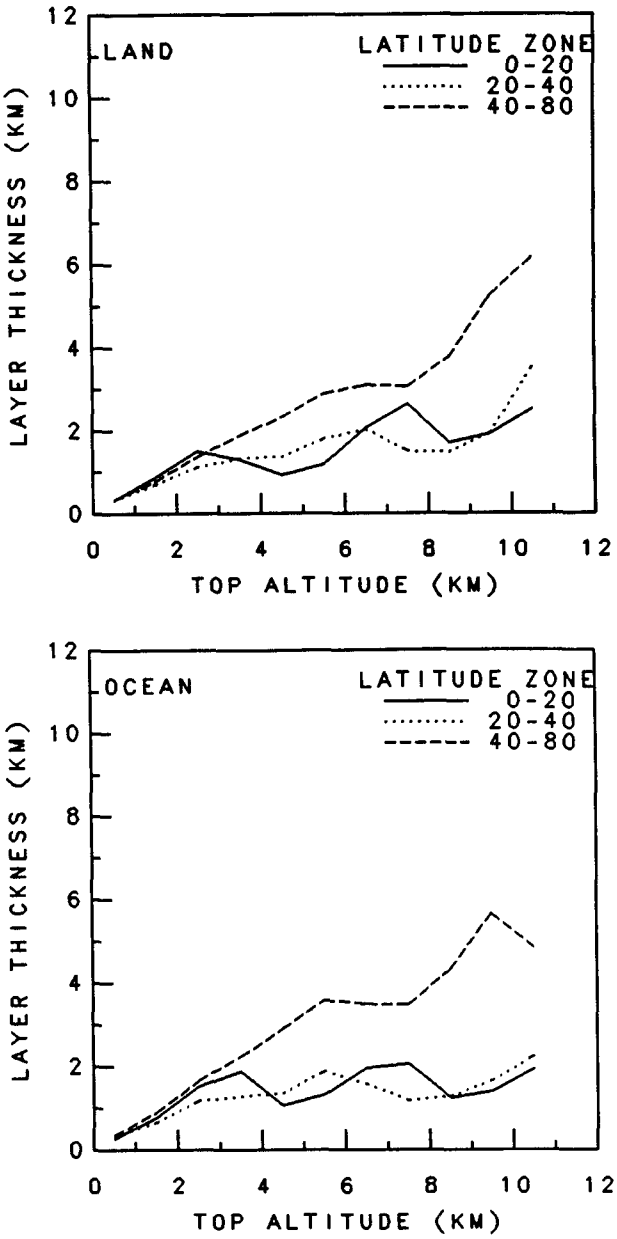

FIG. 14. Variations of average cloud-layer thickness with cloud-top altitude (a) over land and (b) over ocean in three latitude zones: 0°–20°N, 20°–40°N, and 40°–80°N.

periods of record. Better representation of cloud types may be obtained by adjusting the statistics in the CLTC dataset to correspond to the Warren et al. (1986) and Warren et al. (1988) climatology. The effects of incomplete geographic coverage can be determined by matching statistics with a global satellite dataset such as ISCCP (Rossow and Schiffer 1991). To increase the number of multilayer cases, we will need to improve the analysis method as discussed in section 2d. Several objectives might be better met by combining satellite, SWOBS, and RAOBS into one analysis.

Acknowledgments. J. Wang acknowledges support from NSF Grant ATM-9110536 (Determination and Impacts of Surface Radiation Fluxes for TOGA COARE—J. A. Curry, PI). We thank G. Tselioudis and Y.-C. Zhang for useful discussions. We thank A. Walker for computer support.

APPENDIX

Description of 63 Stations

No.	Station ID	Station name	Latitude	Longitude
1	486980	Singapore	1.37°N	103.98°E
2	655780	Abidjan, Ivory Coast	5.25°N	3.93°W
3	913340	Truk Island	7.47°N	151.85°E
4	433690	Minacoy Island	8.30°N	73.00°E
5	612910	Bamako, Mali	12.53°N	7.95°W
6	432950	Bangalore, India	12.97°N	77.58°E
7	789540	Grantly Adams, Bahamas	13.07°N	59.48°W
8	912170	Anderson AFB, Guam	13.55°N	144.83°E
9	616410	Dakar, Senegal	14.73°N	17.50°W
10	483270	Chiang Mai, Thailand	18.78°N	98.98°E
11	766790	Mexico City, Mexico	19.26°N	99.07°W
12	912450	Wake Island	19.28°N	166.65°E
13	912850	Hilo, HI	19.43°N	155.04°W
14	764580	Mazatlan, Mexico	23.18°N	105.42°W
15	419230	Dhaka, Bangladesh	23.77°N	90.38°E
16	722010	Key West, FL	24.33°N	81.45°W
17	479360	Naha, Japan	26.20°N	127.67°E
18	910660	Midway Island	28.13°N	177.22°W
19	600200	Tenerife, Canary Island	28.29°N	16.20°W
20	405820	Kuwait	29.22°N	47.98°E
21	722610	Del Rio, TX	29.37°N	100.92°W
22	605710	Bechar, Algeria	31.63°N	2.25°W
23	722740	Tucson, AZ	32.12°N	110.93°W
24	780160	Bermuda Island	32.37°N	64.68°W
25	722080	Charleston, SC	32.90°N	80.03°W
26	400800	Damascus, Syria	33.42°N	36.52°E
27	723530	Oklahoma City, OK	35.40°N	97.60°W
28	723270	Nashville, TN	36.25°N	86.57°W
29	471220	Osan AB, Korea	37.10°N	127.03°E
30	724930	Oakland, CA	37.73°N	122.20°W
31	167160	Athens, Greece	37.90°N	23.73°E
32	085090	Lajes, Azores	38.73°N	27.08°W
33	725720	Salt Lake, UT	40.46°N	111.58°W
34	725320	Peoria, IL	40.67°N	89.68°W
35	725970	Medford, OR	42.37°N	122.87°W
36	725180	Albany, NY	42.75°N	73.80°W
37	716000	Sable Island, Canada	43.93°N	60.02°W
38	075100	Bordeaux, France	44.83°N	0.70°W
39	160800	Milan, Italy	45.43°N	9.28°E
40	321860	Urup Island, USSR	46.20°N	150.50°E
41	074810	Lyon, France	46.22°N	5.13°E
42	718010	St John's, Canada	47.07°N	52.75°W
43	727970	Quillayute, WA	47.95°N	124.55°W
44	345600	Volgograd, USSR	48.68°N	44.35°E
45	353940	Karaganda, USSR	49.80°N	73.13°E
46	115200	Prague, Czech	50.00°N	14.45°E
47	704540	Adak, AK	51.88°N	176.65°W
48	039530	Valentia, Ireland	51.93°N	10.25°W
49	123300	Poznan, Poland	52.42°N	16.83°E
50	103380	Hannover, Germany	52.47°N	9.70°E
51	718160	Goose Bay, Canada	53.32°N	60.42°W
52	718670	The Pas, Canada	53.97°N	101.10°W
53	296340	Novosibirsk, USSR	55.03°N	82.90°E
54	239210	Ivdel', USSR	60.68°N	60.43°E
55	246410	Viljujsk, USSR	63.77°N	121.62°E
56	040180	Keflavik, Iceland	63.97°N	22.60°W

APPENDIX (*Continued*)

Description of 63 Stations

No.	Station ID	Station name	Latitude	Longitude
57	225500	Archangelsk, USSR	64.58°N	40.50°E
58	702610	Fairbanks, AK	64.82°N	147.87°W
59	710810	Hall Beach, Canada	68.78°N	81.25°W
60	700260	Barrow, AK	71.30°N	156.78°W
61	042020	Thule, Greenland	76.52°N	68.83°W
62	202920	Celjuskin, USSR	77.72°N	104.28°E
63	201070	Barencburg, USSR	78.07°N	14.22°E

REFERENCES

Air Ministry Meteorological Office, 1956: *Observer's Handbook.* Her Majesty's Stationery Office, London, 216 pp.

Arking, A., 1991: The radiative effects of clouds and their impact on climate. *Bull. Amer. Meteor. Soc.,* **71,** 795–813.

AWS, 1979: The use of the skew of *T,* log *P* diagram in analysis and forecasting. AWS/TR-79/006, Air Weather Service, Scott AFB, IL, 150 pp.

Bary, E. D., and F. Moller, 1963: The vertical distribution of clouds. *J. Appl. Meteor.,* **2,** 806–808.

Baum, B. A., R. F. Arduini, B. A. Wielicki, P. Minnis, and S.-C. Tsay, 1994: Multilevel cloud retrieval using multispectral HIRS and AVHRR data: Nighttime oceanic analysis. *J. Geophys. Res.,* **99,** 5499–5514.

Betts, A. K., 1989: Idealized model for stratocumulus cloud layer thickness. *Tellus,* **41A,** 246–254.

Carlson, B. E., A. A. Lacis, and W. B. Rossow, 1993: Tropospheric gas composition and cloud structure of the Jovian North Equatorial Belt. *J. Geophys. Res.,* **98,** 5251–5290.

Cotton, W. R., and R. A. Anthes, 1989: *Storm and Cloud Dynamics,* International Geophysics Series, Vol. 44, Academic Press, 883 pp.

Curry, J. A., C. D. Ardeel, and L. Tian, 1990: Liquid water content and precipitation characteristics of stratiform clouds as inferred from satellite microwave measurements. *J. Geophys. Res.,* **95,** 16 695–16 671.

Elliott, W. P., and D. J. Gaffen, 1991: On the utility of radiosonde humidity archives for climate studies. *Bull. Amer. Meteor. Soc.,* **72,** 1507–1520.

Fung, I. Y., D. E. Harrison, and A. A. Lacis, 1984: On the variability of the net longwave radiation at the ocean surface. *Rev. Geophys. Space Phys.,* **22,** 177–193.

Gaffen, D. J., T. P. Barnett, and W. P. Elliott, 1991: Space and time scales of global tropospheric moisture. *J. Climate,* **4,** 989–1008.

Garand, L., C. Grassotti, J. Halle, and G. L. Klein, 1992: On differences in radiosonde humidity-reporting practices and their implications for numerical weather prediction and remote sensing. *Bull. Amer. Meteor. Soc.,* **73,** 1417–1423.

Hahn, C. J., S. G. Warren, J. London, R. M. Chervin, and R. Jenne, 1982: Atlas of simultaneous occurrence of different cloud types over ocean. NCAR Tech. Note TN-201+STR, National Center for Atmospheric Research, Boulder, 212 pp.

——, ——, ——, ——, and ——, 1984: Atlas of simultaneous occurrence of different cloud types over land. NCAR Tech. Note TN-241+STR, National Center for Atmospheric Research, Boulder, 211 pp.

Henderson-Sellers, A., 1986: Layer cloud amounts for January and July 1979 from 3D-Nephanalysis. *J. Climate Appl. Meteor.,* **25,** 118–132.

Houze, R. A., 1982: Cloud clusters and large-scale vertical motions in the tropics. *J. Meteor. Soc. Japan,* **60,** 396–410.

Hughes, N. A., 1984: Global cloud climatologies: A historical review. *J. Climate Appl. Meteor.,* **23,** 724–751.

Izumi, Y., 1982: A study of cirriform clouds over eleven USSR stations. AFGL-TR-82-0384, Air Force Geophysics Laboratory, Hanscom AFB, MA, 148 pp.

Kahl, J. D., M. C. Serreze, S. Shiotani, S. M. Skony, and R. C. Schnell, 1992: In situ meteorological sounding archives for Arctic studies. *Bull. Amer. Meteor. Soc.,* **73,** 1824–1830.

Kropfli, R. A., and Coauthors, 1995: Studies of cloud microphysics with millimeter wave radar. *Atmos. Res.,* in press.

Liao, X., W. B. Rossow, and D. Rind, 1995a: Comparison between SAGE II and ISCCP high-level clouds, Part I: Global and zonal mean cloud amounts. *J. Geophys. Res.,* in press.

——, ——, and ——, 1995b: Comparison between SAGE II and ISCCP high-level clouds, Part II: Locating cloud tops. *J. Geophys. Res.,* in press.

Liu, W. T., W. Tang, and P. P. Niller, 1991: Humidity profiles over the ocean. *J. Climate,* **4,** 1023–1034.

Machado, L. A. T., and W. B. Rossow, 1993: Structural characteristics and radiative properties of tropical cloud clusters. *Mon. Wea. Rev.,* **121,** 3234–3260.

Minnis, P., D. F. Young, C. W. Fairall, and J. B. Snider, 1992: Stratocumulus cloud properties from simultaneous satellite and island-based instrumentation during FIRE. *J. Appl. Meteor.,* **31,** 317–339.

Morcrette, J.-J., and Y. Fouquart, 1986: The overlapping of cloud layers in shortwave radiation parameterizations. *J. Atmos. Sci.,* **43,** 321–328.

Platt, C. M. R., 1989: The role of cloud microphysics in high-cloud feedback effects on climate change. *Nature,* **341,** 428–429.

——, and Harshvardhan, 1988: Temperature dependence of cirrus extinction: Implications for climate feedback. *J. Geophys. Res.,* **93,** 11 051–11 058.

Poore, K. D., 1991: Cloud base, top and thickness climatology from RAOB and surface data. *Proc. Cloud Impacts on DOD Operations and Systems 1991 Conf.,* Hanscom Air Force Base, Phillips Laboratory, 65–69. [PL-TR-92-2335:]

Rossow, W. B., and A. A. Lacis, 1990: Global, seasonal cloud variations from satellite radiance measurements. Part II: Cloud properties and radiative effects. *J. Climate,* **3,** 1204–1253.

——, and R. A. Schiffer, 1991: ISCCP cloud data products. *Bull. Amer. Meteor. Soc.,* **72,** 2–20.

Sassen, K., 1991: The polarization lidar technique for cloud research: A review and current assessment. *Bull. Amer. Meteor. Soc.,* **72,** 1848–1866.

Schwartz, B. E., and C. A. Doswell III, 1991: North American rawinsonde observations: Problems, concerns, and a call to action. *Bull. Amer. Meteor. Soc.,* **72,** 1885–1896.

Stephens, G. L., and P. J. Webster, 1979: Sensitivity of radiative forcing to variable cloud and moisture. *J. Atmos. Sci.,* **36,** 1542–1556.

——, and ——, 1981: Clouds and climate: Sensitivity of simple systems. *J. Atmos. Sci.,* **38,** 235–247.

——, and ——, 1984: Cloud decoupling of the surface and planetary radiative budgets. *J. Atmos. Sci.,* **41,** 681–686.

Stowe, L. L., H. Y. M. Yeh, T. F. Eck, C. G. Wellemeyer, and H. L. Kyle, 1989: *Nimbus-7* global cloud climatology. Part II: First year results. *J. Climate,* **2,** 671–709.

Tian, L., and J. A. Curry, 1989: Cloud overlap statistics. *J. Geophys. Res.,* **94,** 9925–9935.

Tselioudis, G., and W. B. Rossow, 1994: Global, multiyear variations of optical thickness with temperature in low and cirrus clouds. *Geophys. Res. Lett.,* **21,** 2211–2214.

——, ——, and D. Rind, 1992: Global patterns of cloud optical thickness variation with temperature. *J. Climate,* **5,** 1484–1495.

Warren, S. G., C. J. Hahn, and J. London, 1985: Simultaneous occurrence of different cloud types. *J. Climate Appl. Meteor.,* **24,** 658–667.

——, ——, ——, R. M. Chervin, and R. L. Jenne, 1986: Global distribution of total cloud cover and cloud type amounts over land. NCAR Tech. Note NCAR/TN-273+STR, National Center for Atmospheric Research, Boulder, 29 pp +200 maps.

——, ——, ——, ——, ——, 1988: Global distribution of total cloud cover and cloud type amounts over ocean. NCAR Tech. Note NCAR/TN-317+STR, National Center for Atmospheric Research, Boulder, 42 pp + 170 maps.

WCRP-84, 1994: Utility and feasibility of a cloud profiling radar. Report of the GEWEX topical workshop, WMO/TD-No. 593, World Meteorological Organization, Geneva, 46 pp.

Webster, P. J., and G. L. Stephens, 1984: Cloud-radiation interaction and the climate problem. *The Global Climate,* J. Houghton, Ed., Cambridge University Press, 63–78.

Woodbury, G. E., and M. P. McCormick, 1986: Zonal and geographical distributions of cirrus cloud determined from SAGE data. *J. Geophys. Res.,* **91,** 2775–2785.

Zhang, Y.-C., W. B. Rossow, and A. A. Lacis, 1995: Calculation of surface and top-of-atmosphere radiative fluxes from physical quantities based on ISCCP datasets, Part I: Method and sensitivity to input data uncertainties. *J. Geophys. Res.,* in press.